Large-scale calculation of optical dielectric functions of diamond nanocrystallites

Yoshiyuki Kurokawa
Doctoral Program in Engineering, University of Tsukuba, Tsukuba 305-8573, Japan

Shintaro Nomura
Institute of Physics, University of Tsukuba, Tsukuba 305-8571, Japan

Tadashi Takemori
Institute of Materials Science, University of Tsukuba, Tsukuba 305-8573, Japan

Yoshinobu Aoyagi
RIKEN, 2-1 Hirosawa, Wako, Saitama 351-0198, Japan

(Received 27 December 1999)

The real-time real-space higher-order finite-difference method is applied to the calculation of dielectric functions of diamond crystallites. The calculation is performed for cubic grains of various sizes, the largest of which is of 4-nm linear dimension and contains 13 460 carbon atoms. The surface dangling bonds are terminated with hydrogen atoms, and empirical pseudopotentials are used for the two types of atoms. The shift of the absorption peak with the crystallite size is a manifestation of the quantum size effect.

The quantum size effect in semiconductor nanocrystallites has been a focus of attention during recent years, and there is now a good body of work, both experimental[1] and theoretical,[2] on the effect in nanocrystallites of conventional semiconductor materials such as Si, GaAs, GaP, InP, and CdSe. In comparison, research on diamond nanocrystallites has been relatively slow despite the special interest in the material because of the potential applications stemming from the larger band gap and the resulting robustness. However, the recent development of novel techniques of diamond crystallite production, such as the deposition growth of thin films[3–5] and the detonation synthesis from explosives,[6–9] has greatly facilitated the controlled preparation of diamond particles, and experimental results are beginning to accumulate for diamond nanocrystallites.[4,7,8] In particular, extensive studies using x-ray crystallography[7] and Raman spectroscopy[7,8] have led to reliable methods of sample characterization.

Through such investigations, it has come to be realized that the particle size of such diamond powder lies typically in the range 3–6 nm. This is drawing special attention because quantum size effects should be readily observable in crystallites of such sizes. For example, the characteristic features of the Raman scattering spectra of explosion diamonds are explained in terms of size quantization of the phonon spectrum and the influence of spatial confinement on the photon-phonon interaction.[9] Very recently, x-ray spectroscopy of a series of nanodiamond thin films has revealed resonant peaks that resemble the carbon $1s$ core exciton absorption, and the exciton state and the conduction-band edge are both found to shift to higher energies with the decrease of the grain size.[5]

In the light of the accumulation of such experimental data, one would like to have the theoretical calculation based on a realistic model of the crystallites. However, the calculation rapidly becomes intractable as the number of atoms N in the model increases. If one uses the pseudopotential for the electron binding potential and solves for energy eigenvalues and eigenstates using the standard diagonalization method, the memory requirement and the CPU time grow as $O(N^2)$ and $O(N^3)$, respectively. This can easily overwhelm the capacity of the largest computing facility with N in the thousands for diamond nanocrystallites. The real-time real-space higher-order finite-difference method[10–13] is an $O(N)$ method that requires both the memory space and the CPU time only in proportion to the system size N. The real space is represented by a set of discrete mesh points, and the time development of a system is solved by numerically integrating the Schrödinger equation for discrete time steps. The powerfulness of this method has been demonstrated in the calculation of the optical-absorption spectra of hydrogenated silicon nanocrystallites[11,14] and silicon nanocrystals embedded in amorphous silicon,[12] where the models contained more than 10 000 Si atoms. The algorithm was recently applied also to the calculation of nonlinear response functions.[13]

In this paper we report a further application of the method to the calculation of the linear dielectric function of hydrogenated diamond nanocrystallites containing as many as 13 460 carbon atoms. The model is that of a system of noninteracting electrons that are trapped by the atomic potential of carbon and hydrogen, and we use the empirical pseudopotential for both types of atoms.

In the real-time real-space higher-order finite-difference method, the electronic density of states $\rho(\omega)$ and the complex dielectric function $\epsilon_{\beta\alpha}(\omega)$ are given by[10]

$$\rho(\omega)=-\frac{1}{\pi}\mathrm{Im}\left\langle \frac{1}{i\hbar}\int_0^T dt e^{i(\omega+i\eta)t}\langle\Phi|e^{-iHt}|\Phi\rangle \right\rangle_{\Phi} \quad (1)$$

and

$$\epsilon_{\beta\alpha}(\omega)=\delta_{\beta\alpha}+4\pi\left\langle \int_0^T dt e^{-\eta t}(e^{i\omega t}-\delta_{\beta\alpha})K_{\beta\alpha}(t) \right\rangle_{\Phi}, \quad (2)$$

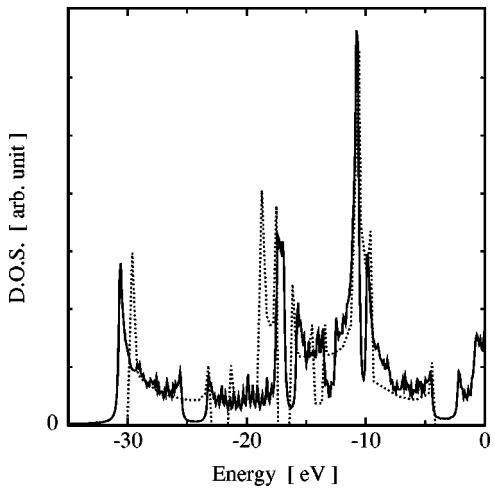

FIG. 1. Density of states of *trans*-polyacetylene. Our calculation is indicated by the solid line and VEH calculation of Ref. 21 is shown by the dotted line.

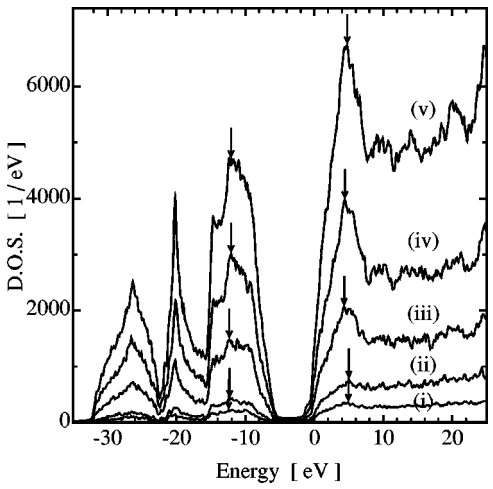

FIG. 2. Density of states of hydrogenated carbon nanocrystallites: (i) $C_{528}H_{294}$, (ii) $C_{1050}H_{498}$, (iii) $C_{4048}H_{1182}$, (iv) $C_{8120}H_{1950}$, and (v) $C_{13464}H_{2730}$.

where

$$K_{\beta\alpha}(t)=\frac{-2}{V(\omega+i\eta)}\mathrm{Im}\langle\Phi|\,\theta(E_F-H)e^{iHt}\mathbf{p}_\beta e^{-iHt}\times\theta(E_{cut}-H)\,\theta(H-E_F)\mathbf{p}_\alpha|\Phi\rangle. \quad (3)$$

Here, the suffixes α and β are the spatial index x, y, or z. The spectral energy resolution is specified by η in Eqs. (1) and (2), and the total time of integration T is set to satisfy $e^{-\eta T}<\delta$, where δ is the required relative numerical accuracy which is set to 0.01 in the present calculation. The symbols H, V, $\theta(H)$, $\mathbf{p}_\alpha$ and E_F in Eq. (3) stand for the Hamiltonian of the system, the volume of the system, the operator step function, the momentum operator, and the Fermi energy, respectively. The differential operators in the Hamiltonian are approximated by the discretized form of the higher-order finite-difference method of order 2.[15] The time development e^{-iHt} is solved by numerically integrating the Schrödinger equation. The operator step function $\theta(X)$ can be explicitly constructed for any bounded Hermitian operator X without solving for its eigenvalues and eigenvectors.[16] In our calculation, we use an algorithm based on the Chebyshev polynomial expansion, which yields $\theta(X)$ as a polynomial of the operator X.[10,11,16,17] The insertion of $\theta(E_{cut}-H)$ is necessary to eliminate the statistical fluctuations originating from the unphysical high-energy components. The state $|\Phi\rangle$ in Eqs. (1)–(3) is the random-phase vector[10] whose amplitude at lattice points in space is $e^{i\theta}$ with the phase θ being a random variable drawn independently for each lattice site from the uniform distribution in the range $[-\pi,\pi)$. We represent the three-dimensional real space by a uniform cubic grid of $N_x\times N_y\times N_z$ points so that the random vector $|\Phi\rangle$ is a column vector of dimension $N_xN_yN_z$. Using the completeness property of the random-phase vector $|\Phi\rangle$, the trace of an operator $\hat{O}$ is obtained by taking the statistical average of $\langle\Phi|\hat{O}|\Phi\rangle$ over the random realizations of $|\Phi\rangle$.[16] Since this averaging, indicated by $\langle\cdots\rangle_\Phi$ in Eqs. (1) and (2), converges fast when the dimension of the random-phase vector is large, the dependence of the computation cost on the system size is sublinear.[17] In fact, for the features corresponding to bulk properties of the crystallites, the total CPU time to achieve the same level of statistical convergence is practically independent of the system size.

We construct the electron binding potential as a superposition of empirical pseudopotentials[18] of carbon atoms and hydrogen atoms. For the carbon pseudopotential, we adopt the simple procedure of scaling the potential used for Si in Ref. 19. The Fourier transform of the potential then has the analytical form $V_C(k)=\lambda(\mu k^2-\chi)/(e^{\mu k^2-\nu}+1)$. The band calculation with this potential reproduces the qualitative features of the diamond band structure near the Fermi energy. We achieve quantitative agreement by adjusting the scaling factors λ and μ by the least-squares method to fit three vertical transition energies $\Delta E(\Gamma_{25}'\rightarrow\Gamma_2)$, $\Delta E(X_4\rightarrow X_1)$, and $\Delta E(L_3'\rightarrow L_3)$ to the values 8.22, 11.79 and 13.13 eV taken from the nonlocal pseudopotential band calculation.[20] This gives $\lambda=1.781,\chi=1.424,\mu=0.354$, and $\nu=0.938$ in atomic units with the transition energies $\Delta E(\Gamma_{25}'\rightarrow\Gamma_2)=8.23$ eV, $\Delta E(X_4\rightarrow X_1)=11.68$ eV, and $\Delta E(L_3'\rightarrow L_3)=13.23$ eV. The pseudopotential for the hydrogen atom has also to be scaled from the one used in Ref. 19 in order for surface levels to appear at correct energies. This we do by applying an overall multiplicative factor to the hydrogen potential used in Ref. 19, so as to reproduce the electronic density of states of *trans*-polyacetylene near the Fermi level when used in combination with the carbon pseudopotential. We show the result in Fig. 1 together with the density of states obtained with the valence effective Hamiltonian (VEH) method.[21] By requiring that there be no structure in the main energy gap at -3.5 eV, and that the largest peak near -10 eV appear at the correct energy, the pseudopotential in the momentum space is determined in atomic units as $V_H(k)=-0.397+0.0275k+0.1745k^2-0.0531k^3$ for $k\leqslant 2$ and $V_H(k)=0.0811/k-1.086/k^2+2.71/k^3-2.86/k^4$ for $k>2$.

As for the spatial structure of a diamond nanocrystallite, we take the model of a cubic block cut out of a perfect diamond. The study of the conduction electron suggests that carbon atoms take a configuration similar to that of the bulk diamond for crystallites of more than 4300 atoms.[5] In the

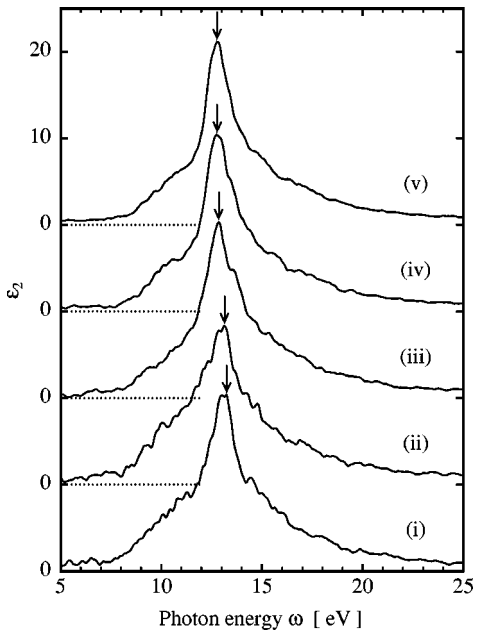

FIG. 3. The imaginary part of the dielectric function of hydrogenated carbon nanocrystals: (i) $C_{528}H_{294}$, (ii) $C_{1050}H_{498}$, (iii) $C_{4048}H_{1182}$, (iv) $C_{8120}H_{1950}$, and (v) $C_{13464}H_{2730}$.

absence of detailed knowledge of atomic arrangements for smaller crystallites, here we assume the tetrahedral configuration of the bulk diamond crystal irrespective of the crystallite size. The surface dangling bonds are terminated with hydrogen atoms placed in the direction of the tetrahedral bonds at a distance 0.111 nm from the carbon atom to correspond to the average C-H bond length of the CH_4 molecule at room temperature.[22] The wave functions are solved under the boundary condition that they vanish on the faces of the cubic volume containing the crystallite. In all calculations, the volume boundaries are placed more than 0.35 nm away from the outermost hydrogen atoms to ensure that the boundary condition does not interfere with the physical results.

Figure 2 shows the density of states calculated for cubic hydrogenated carbon nanocrystallites $C_{528}H_{294}$, $C_{1050}H_{498}$, $C_{4048}H_{1182}$, $C_{8120}H_{1950}$, and $C_{13464}H_{2730}$ with faces (110), $(1\bar{1}0)$, and (001). The size of the cubic spatial grid used in these calculations to represent the three-dimensional space varies from $96\times96\times96=884\,736$ points to $240\times240\times240=13\,824\,000$ points, and the set of two to eight random vectors are used for statistical averaging, depending on the size of the nanocrystallites. The energy resolution η and the cutoff energy E_{cut} are set to 100 meV and 100 eV, respectively. The finite value of the density of states inside the gap region is the accumulated Lorentzian tails of the resolution function and diminishes at higher resolution. The characteristic peaks

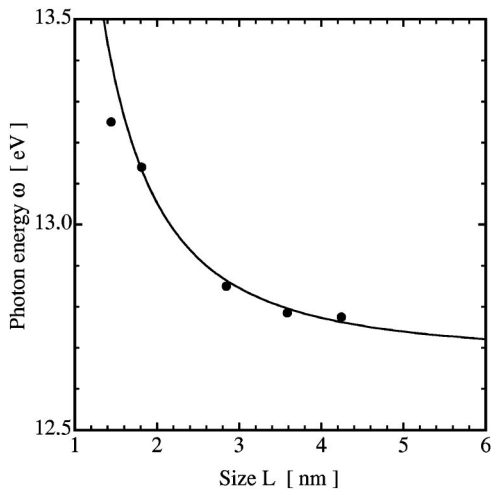

FIG. 4. Size dependence of the peak position indicated by arrows in Fig. 3. The solid line shows the curve $\omega=12.68+1.49L^{-2}$ for comparison.

indicated by arrows in Fig. 2 move away from the band gap with decreasing size of the nanocrystallite.

The size effect is also evident in the dielectric function whose imaginary part $\mathcal{E}_2$ is shown as a function of the photon energy ω for various grain sizes in Fig. 3. The energy resolution is set to $\eta=120$ meV. The position of the peak shown by the arrows in Fig. 3 is plotted against the linear dimension L of the crystallite in Fig. 4. While the nature of the peak shift with the crystallite size is unclear, the shift is a clear manifestation of the quantum size effect. We have drawn a curve $\omega=12.68+1.49L^{-2}$ in the figure for comparison.

In conclusion, we have applied the real-time real-space higher-order finite-difference method to hydrogenated carbon nanocrystallites of various sizes, and obtained the absorption spectra that vary with the crystallite size. The present calculation may be improved upon in various ways; more sophisticated local or nonlocal pseudopotentials may be used for the two types of atoms, and the atomic rearrangement and the lattice relaxation near the grain surface may be taken into account if the necessary data becomes available. However, certain qualitative features of the absorption spectrum and their variation with the crystallite size seen in the present calculation may find their counterparts in actual measurements on diamond crystallites. It is hoped that with feedback from experiment and with refinement of the potentials, qualitative comparison will eventually be made to clarify the nature of various phenomena observed in diamond nanocrystallites.

All calculations reported here were performed on a Fujitsu VPP700 at RIKEN.

[1] T. van Buuren, Y. Gao, T. Tiedje, J.R. Dahn, and B.M. Way, Appl. Phys. Lett. **60**, 3013 (1992); T. van Buuren, L.N. Dinh, L.L. Chase, W.J. Siekhaus, and L.J. Terminello, Phys. Rev. Lett. **80**, 3803 (1998); P.E. Batson and J.R. Heath, *ibid.* **71**, 911 (1993); Y. Wang and N. Herron, Phys. Rev. B **42**, 7253 (1990).

[2] Y. Kayanuma, Phys. Rev. B **38**, 9797 (1988); P.E. Lippens and M. Lannoo, *ibid.* **39**, 10 935 (1989); M.V. Rama Krishma and R.A. Friesner, J. Chem. Phys. **95**, 8309 (1991); A. Tamasulo and M.V. Rama Krishma, *ibid.* **105**, 3612 (1996); L.W. Wang and A. Zunger, Phys. Rev. B **53**, 9579 (1996); A. Mizel and M.L. Co-

hen, *ibid.* **56**, 6737 (1997).
[3] J. Lee, B. Hong, R. Messier, and R.W. Collins, Appl. Phys. Lett. **69**, 1716 (1996).
[4] M.M. Garcia, I. Jimenez, L. Vazquez, C. Gomez-Aleixandre, J.M. Albella, O. Sanchez, L.J. Terminello, and F.J. Himpsel, Appl. Phys. Lett. **72**, 2105 (1998).
[5] Y.K. Chang, H.H. Hsieh, W.F. Pong, M.H. Tsai, F.Z. Chien, P.K. Tseng, L.C. Chen, T.Y. Wang, K.H. Chen, D.M. Bhusari, J.R. Yang, and S.T. Lin, Phys. Rev. Lett. **82**, 5377 (1999).
[6] A.I. Lyamkin, E.A. Petrov, A.P. Ershov, G.V. Sakivich, A.M. Staver, and V.M. Titov, Dokl. Akad. Nauk SSSR **302**, 611 (1998) [Sov. Phys. Dokl. **33**, 705 (1988)]; S.N. Mikov, A.V. Igo, and V.S. Goreliki, Fiz. Tverd. Tela (St. Petersburg) **41**, 1110 (1999) [Phys. Solid State **41**, 1012 (1999)].
[7] M. Yoshikawa, Y. Mori, H. Obata, N. Maegawa, G. Katagiri, H. Ishida, and A. Ishitani, Appl. Phys. Lett. **67**, 694 (1995).
[8] S.N. Mikov, A.V. Igo, and V.S. Gorelik, Fiz. Tverd. Tela (St. Petersburg) **37**, 908 (1995) [Phys. Solid State **37**, 1671 (1995)].
[9] V.S. Gorelik, A.V. Igo, and S.N. Mikov, Zh. Éksp. Teor. Fiz. **109**, 1158 (1996) [JETP **82**, 1154 (1996)].
[10] T. Iitaka, S. Nomura, H. Hirayama, X. Zhao, Y. Aoyagi, and T. Sugano, Phys. Rev. E **56**, 1222 (1997).
[11] S. Nomura, T. Iitaka, X. Zhao, T. Sugano, and Y. Aoyagi, Phys. Rev. B **56**, 4348 (1997).
[12] S. Nomura, T. Iitaka, X. Zhao, T. Sugano, and Y. Aoyagi, Phys. Rev. B **59**, 10 309 (1999).
[13] Y. Kurokawa, S. Nomura, T. Takemori, and Y. Aoyagi, Phys. Rev. E **59**, 3694 (1999).
[14] S. Nomura, X. Zhao, Y. Aoyagi, and T. Sugano, Phys. Rev. B **54**, 13 974 (1996).
[15] J. Chelikowsky, N. Troullier, and Y. Saad, Phys. Rev. Lett. **72**, 1240 (1994).
[16] O.F. Sankey, D.A. Drabold, and A. Gibson, Phys. Rev. B **50**, 1376 (1994).
[17] R.N. Silver and H. Roeder, Int. J. Mod. Phys. C **5**, 735 (1994).
[18] M. L. Cohen and J. R. Chelikowsky, *Electronic Structure and Optical Properties of Semiconductors*, 2nd ed. (Springer-Verlag, Berlin, 1988).
[19] L.W. Wang and A. Zunger, J. Chem. Phys. **100**, 2394 (1994).
[20] L.A. Hemstreet, Jr., C.Y. Fong, and M.L. Cohen, Phys. Rev. B **2**, 2054 (1970).
[21] J.L. Bredas, R.R. Chance, R. Silbey, G. Nicolas, and Ph. Durand, J. Chem. Phys. **75**, 255 (1981).
[22] *Zahlenwerte und Funktionen aus Naturwissenschaften und Technik*, edited by J. H. Callomon, E. Hirota, K. Kuchitsu, W. J. Lafferty, A. G. Maki, and C. S. Pote, Landolt-Börnstein, New Series, Group II, Vol. 7 (Springer, New York, 1976); L.S. Bartell, K. Kuchitsu, and R.J. deNeui, J. Chem. Phys. **35**, 1211 (1961).